

Ganglion-specific splicing of TRPV1 underlies infrared sensation in vampire bats

Elena O. Gracheva^{1*}, Julio F. Cordero-Morales^{1*}, José A. González-Carcacia², Nicholas T. Ingolia³, Carlo Manno⁴, Carla I. Aranguren², Jonathan S. Weissman^{5,6,7} & David Julius^{1,5}

Vampire bats (*Desmodus rotundus*) are obligate blood feeders that have evolved specialized systems to suit their sanguinary lifestyle^{1–3}. Chief among such adaptations is the ability to detect infrared radiation as a means of locating hotspots on warm-blooded prey. Among vertebrates, only vampire bats, boas, pythons and pit vipers are capable of detecting infrared radiation^{1,4}. In each case, infrared signals are detected by trigeminal nerve fibres that innervate specialized pit organs on the animal's face^{5–10}. Thus, vampire bats and snakes have taken thermosensation to the extreme by developing specialized systems for detecting infrared radiation. As such, these creatures provide a window into the molecular and genetic mechanisms underlying evolutionary tuning of thermoreceptors in a species-specific or cell-type-specific manner. Previously, we have shown that snakes co-opt a non-heat-sensitive channel, vertebrate TRPA1 (transient receptor potential cation channel A1), to produce an infrared detector⁶. Here we show that vampire bats tune a channel that is already heat-sensitive, TRPV1, by lowering its thermal activation threshold to about 30 °C. This is achieved through alternative splicing of TRPV1 transcripts to produce a channel with a truncated carboxy-terminal cytoplasmic domain. These splicing events occur exclusively in trigeminal ganglia, and not in dorsal root ganglia, thereby maintaining a role for TRPV1 as a detector of noxious heat in somatic afferents. This reflects a unique organization of the bat *Trpv1* gene that we show to be characteristic of Laurasiatheria mammals (cows, dogs and moles), supporting a close phylogenetic relationship with bats. These findings reveal a novel molecular mechanism for physiological tuning of thermosensory nerve fibres.

Vampire bats have three 'leaf pits' that surround the nose (Fig. 1a) and receive input from low-threshold heat-sensitive nerve fibres responding to stimuli at temperatures >29 °C (refs 1, 7, 11, 12). Closely related fruit bats (*Carollia brevicauda*) have a different nasal structure devoid of pit organs (Fig. 1a) and thus cannot detect infrared stimuli³. Sensory ganglia of fruit bats showed a typical size distribution of neurons resembling that seen in other mammals (Fig. 1b). In contrast, trigeminal ganglia (TG) from vampire bats showed marked skewing towards large diameter neurons, much like that observed in TG of pit-bearing snakes⁶, suggesting that anatomical specialization of TG in vampire bats has similarly evolved to suit a predominant role in infrared sensation. Consistent with this, vampire bat dorsal root ganglia (DRG) showed a normal size distribution, resembling sensory ganglia of fruit bats or other mammals (Fig. 1b). To our knowledge, vampire bats provide the only such example of TG specialization among mammalian species.

Given the distinct anatomy of vampire bat TG versus DRG, we asked whether these ganglia show differential patterns of gene expression that might highlight molecules specifically involved in infrared sensation, as in the case of infrared-sensing snakes⁶. Thus, we performed 'deep sequencing' of complementary DNAs from bat TG and DRG.

Initially, transcriptomes from these ganglia appeared to be indistinguishable (Supplementary Fig. 1). However, examination of cDNAs encoding candidate thermosensors revealed a novel short isoform of the capsaicin receptor, TRPV1, an excitatory ion channel that is activated by noxious heat (>43 °C) (refs 13–15). This isoform (TRPV1-S) lacks 62 amino acids from the carboxy terminus (Fig. 2a and Supplementary Fig. 2) and is uniquely expressed in TG from vampire bat, constituting between 35% and 46% of all TRPV1 transcripts in TG, but <3% in DRG, as determined from transcriptome data or direct cloning and sequencing of RT-PCR (PCR of reverse transcripts) products amplified from sensory ganglia (Fig. 2b). Moreover, TRPV1-S transcripts were barely detected (<6%) in fruit bat TG or DRG

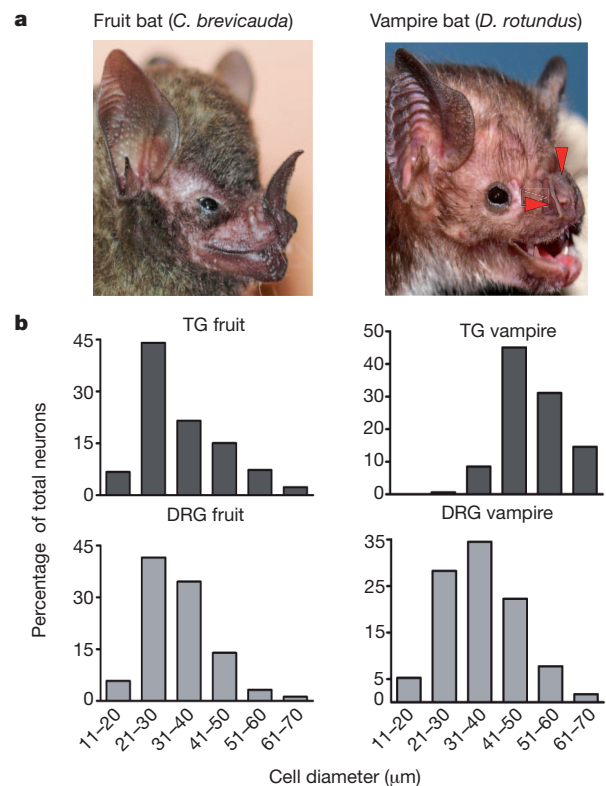


Figure 1 | Anatomy of fruit bat and vampire bat sensory ganglia. **a**, Facial anatomy of fruit bat (left) and vampire bat (right). Red arrowheads mark pit organs surrounding the vampire bat's nose. **b**, Neuronal cell sizes determined from histological sections of fruit bat TG ($n = 300$, 7 independent sections), fruit bat DRG ($n = 345$, 9 sections), vampire bat TG ($n = 164$, 6 sections) and vampire bat DRG ($n = 400$, 11 sections).

¹Department of Physiology, University of California, San Francisco, California 94158-2517, USA. ²Centro de Ecología, Laboratorio de Biología de Organismos, Instituto Venezolano de Investigaciones Científicas (IVIC), Caracas 1020-A, Venezuela. ³Department of Embryology, Carnegie Institution, Baltimore, Maryland 21218, USA. ⁴Centro de Biofísica y Bioquímica, Laboratorio de Fisiología Celular, Instituto Venezolano de Investigaciones Científicas (IVIC), Caracas 1020-A, Venezuela. ⁵Department of Cellular and Molecular Pharmacology, University of California, San Francisco, California 94158-2517, USA. ⁶California Institute for Quantitative Biosciences, University of California, San Francisco, California 94158-2517, USA. ⁷Howard Hughes Medical Institute, University of California, San Francisco, California 94158-2517, USA.

*These authors contributed equally to this work.

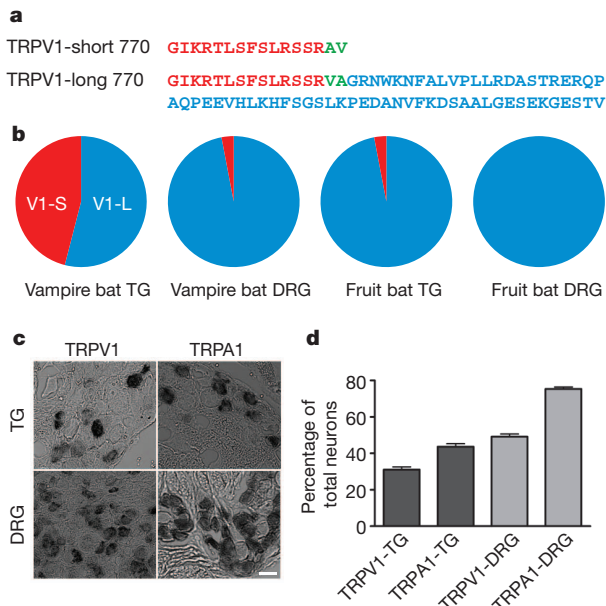


Figure 2 | Sequence and distribution of vampire bat TRPV1. **a**, Deduced protein sequences for TRPV1 short (TRPV1-S) and long (TRPV1-L) isoforms from vampire bat sensory ganglia. **b**, Abundance of TRPV1 isoform transcripts in vampire and fruit bat sensory ganglia as determined by transcriptome profiling and/or direct sequencing of RT-PCR products (≥ 86 clones) amplified from sensory ganglia mRNA. **c**, *In situ* hybridization, showing expression of TRPV1 and TRPA1 transcripts in histological sections from vampire bat TG or DRG (scale bar, 50 μm). **d**, Prevalence of TRPV1 or TRPA1 mRNA expression within vampire bat TG or DRG (mean \pm s.e.m.). Data derived from $n = 554$ neurons, 14 sections for V1-TG; 783 neurons, 17 sections for A1-TG; 1,455 neurons, 15 sections for V1-DRG; and 1,030 neurons, 10 sections for A1-DRG.

(Fig. 2b), and represented $\leq 1.8\%$ of TRPV1 transcripts from TG of three other fruit, nectar or insect feeding bat species (*Uroderma bilobatum*, *Sturnira lilium* and *Anoura cultrata*). Taken together, these observations support the notion that TRPV1-S contributes to the

specialized function of vampire bat TG, most notably infrared sensation.

Discrete cellular expression of TRPV1 in vampire bat sensory ganglia was confirmed by *in situ* hybridization. Consistent with deep sequencing analysis, TRPV1 transcripts were found in similar percentages of TG and DRG neurons ($31.1 \pm 1.5\%$ and $49.2 \pm 1.5\%$, respectively) (Fig. 2c, d). Specificity of this pattern was confirmed by examining the distribution of TRPA1 transcripts, which were present in a larger percentage of TG and DRG neurons ($43.6 \pm 1.7\%$ and $75.4 \pm 1.0\%$, respectively) compared to TRPV1 (Fig. 2c, d and Supplementary Fig. 3).

If TRPV1-S contributes to infrared detection in vampire bats, then this isoform should have appropriate temperature sensitivity. We expressed and characterized TRPV1-S and TRPV1-L in HEK293 cells or *Xenopus* oocytes using calcium imaging or electrophysiological assays, respectively. Indeed, we observed a marked difference in temperature sensitivity, such that the TRPV1-S isoform was activated at a substantially lower threshold compared to TRPV1-L ($30.5 \pm 0.7^\circ\text{C}$ versus $39.6 \pm 0.4^\circ\text{C}$ in HEK293 cells, and $31.2 \pm 1.5^\circ\text{C}$ versus $40.2 \pm 0.7^\circ\text{C}$ in oocytes) (Fig. 3a–c and Supplementary Figs 4, 5). Similar thresholds were observed for fruit bat TRPV1 isoforms (Supplementary Figs 4, 6). This $\sim 10^\circ\text{C}$ threshold differential between TRPV1-S and TRPV1-L, together with unique expression of the short isoform in vampire bat TG, is consistent with a role for TRPV1-S in infrared detection. In contrast, heterologously expressed TRPA1 channels from either bat species were heat insensitive (Supplementary Fig. 7).

Our histological analysis does not allow us to discriminate between TRPV1 isoforms. We therefore considered whether their co-expression would produce channels having lowered thermal thresholds compared to TRPV1-L alone. Injection of oocytes with equal amounts of TRPV1-S and TRPV1-L RNAs produced an intermediate temperature response curve with an activation threshold of $33.9 \pm 1.2^\circ\text{C}$ (Supplementary Fig. 5), rather than biphasic thresholds, suggesting that short and long isoforms can produce functional heterotetrameric complexes. Oocytes expressing mostly one isoform (10S:1L or 1S:10L) showed a thermal threshold defined by the predominant species (Supplementary Fig. 5). Thus, if individual TG neurons express equivalent levels of short and long isoforms, then they will have lower thermal thresholds compared to cells predominately expressing the long form.

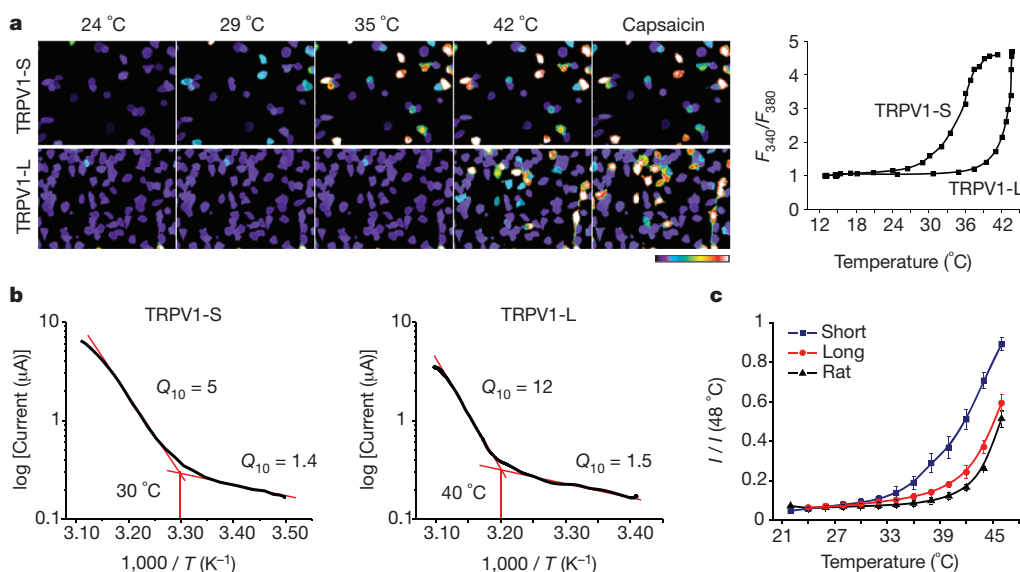


Figure 3 | Functional analyses of vampire bat TRPV1 isoforms. **a**, HEK293 cells expressing vampire bat TRPV1 isoforms were analysed for heat or capsaicin (10 μM)-evoked responses using calcium imaging; colour bar indicates relative change in fluorescence ratio, with purple and white denoting lowest and highest cytoplasmic calcium, respectively ($n \geq 141$ cells per channel). Average temperature-response profiles for capsaicin-sensitive cells

are shown at right. **b**, Arrhenius plots show thermal thresholds and Q_{10} values for baseline and evoked responses for TRPV1-S and TRPV1-L (+80 mV, $n = 8$). **c**, Relative heat response profiles of vampire bat TRPV1 isoforms compared with rat TRPV1, as measured electrophysiologically in oocytes (response at each temperature was normalized to maximal response at 48°C ; $V_H = -80$ mV, $n \geq 8$). Data show mean \pm s.d.

The identification of C-terminal TRPV1 splice variants in vampire bats is somewhat surprising because, to our knowledge, such isoforms have not been previously reported for other species. Alignment between vampire bat TRPV1-S and -L cDNAs highlighted a 23-base-pair insertion in the former (Supplementary Fig. 8a) containing a stop codon that accounts for production of the short isoform. We used sequences flanking this insert to amplify and characterize the organization of the vampire bat *Trpv1* locus in this vicinity. The resulting 5.5-kilobase (kb) fragment contained a tiny 23-base-pair exon (14a) flanked by two introns (2.1 and 3.1 kb), each marked by canonical –GT/AG– donor-acceptor sites required for U2-dependent splicing, as well as obligate polypyrimidine tracts preceding potential splicing sites^{16,17}, allowing for formation of two splice variants that incorporate or bypass exon 14a to produce TRPV1-S or TRPV1-L, respectively (Supplementary Fig. 9).

To determine whether exon 14a-based splicing is a hallmark of other Laurasiatheria orders, we carried out transcriptome and/or genomic analysis from Cetartiodactyla (cow, pig), Carnivora (dog) and Lipotyphla (coast mole), as well as several additional bat species representing both Chiroptera suborders, including microbats and megabats^{18–20}. Two types of TRPV1 splicing events can occur (Fig. 4a): in microbats, megabats and moles, exon 14a contains a premature stop

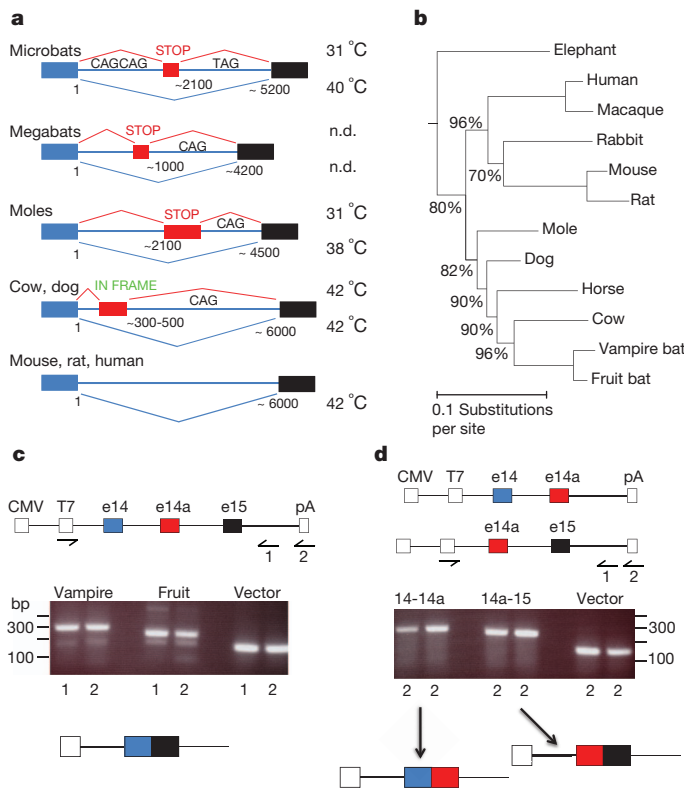


Figure 4 | Genomic organization of mammalian *Trpv1* locus. **a**, Schematic of *Trpv1* gene locus spanning putative exons 14 and 15 in animals of Laurasiatheria, Rodentia and Primate groups. Splicing events between exons 14 (blue) and 15 (black) are shown, including those involving exon 14a (red). Thermal activation thresholds for resulting channel isoforms are shown at right (n.d., not determined). Lengths of intronic region and relative positions of exon 14a are indicated. **b**, Consensus phylogenetic tree from Bayesian estimation, with clade credibility values shown for branches with <100% support. **c, d**, Structures of mini-genes (top) used for *in vivo* splicing assay in HEK293 cells, showing location of CMV promoter and polyadenylation site (pA), defining start and end of transcribed unit. Reverse transcripts were generated with primers annealing to 3' vector sequence (1) or oligo-dT (2), as indicated, and products amplified with T7 and primer (1) pair. Reaction products were resolved on agarose gel (middle) and major bands collected for characterization of splicing products (bottom).

codon accounting for production of a low-threshold TRPV1-S isoform (Supplementary Figs 4–6 and 10). In cows, pigs and dogs, exon 14a produces an in-frame insertion generating an extra-large isoform (TRPV1-XL). Thus, although members of the Laurasiatheria superorder exploit the same intronic region for TRPV1 modification, different suborders show distinct sequences and positions of exon 14a (relative to exons 14 and 15), indicative of independent evolutionary events leading to modification of this intronic region. Interestingly, the architecture of splice sites in microbats differs from that of other Laurasiatheria members, in that the pyrimidine-rich tract is followed by a strong tandem splice site (CAGCAG), and a weak exon 15 acceptor site (TAG in microbats versus CAG in most other species) (Fig. 4a). Consistent with our failure to observe TRPV1-S-like isoforms in mouse sensory ganglia (not shown), neither rodent nor human *TRPV1* gene contains an exon 14a equivalent, limiting splicing to a single isoform.

Although cows and moles have the potential to produce TRPV1 splice variants, we found that <6% of TRPV1 transcripts corresponded to TRPV1-XL or TRPV1-S in TG of cow or mole, respectively, indicating that this form of post-transcriptional regulation is not physiologically relevant in these animals. In cows, this is further underscored by the fact that TRPV1-L and TRPV1-XL isoforms are indistinguishable in regard to thermal response profiles (thresholds of 43.0 ± 0.8 °C and 42.7 ± 0.4 °C, respectively) (Supplementary Figs 4 and 11). Our analysis of *Trpv1* gene organization in different orders (including Chiroptera, Cetartiodactyla, Carnivora, Lipotyphla, Afrotheria and Rodentia) (Fig. 4b and Supplementary Figs 9 and 12) is consistent with an independent molecular phylogeny of mammals^{21,22} and supports the conclusion that bats are more closely related to cows, moles and dogs^{19,20}, rather than to rodents (as initially posited on the basis of anatomical and morphological criteria²³).

Trpv1 genomic sequences for vampire and other microbats in the vicinity of exon 14–14a–15 splice junctions are highly conserved (>90% identity). We therefore asked whether differential splicing was observed when mini-genes containing these genomic regions were introduced into HEK293 cells. Direct splicing of exon 14 to 15, with exclusion of exon 14a, was observed in all cases (Fig. 4c). In mini-gene constructs where direct splicing between exon 14 and 15 was not possible, splicing to or from exon 14a was readily observed (Fig. 4d), indicating that exon 14a is competent to engage in splicing, but disfavoured by exon 14–15 competition. These results show that vampire and fruit bat genes exhibit the same default pattern of exon 14 to 15 splicing in this non-neural context, irrespective of small differences in gene structure. Indeed, this ‘constitutive’ splicing pattern predominates in vampire bat DRG, fruit bat TG and DRG, as well as cow and mole TG, suggesting that efficient splicing to exon 14a in vampire bat TG requires a specialized environment. Furthermore, we have used this assay to identify a putative exon 14a from megabat species, such as *Pteropus vampyrus*, where transcriptome data are not available (Fig. 4a and Supplementary Fig. 13).

Our findings suggest that variation within the TRPV1 C-terminus represents a genetic mechanism for tuning the thermal response profile of the channel in a species- or tissue-specific manner. We therefore asked whether more primitive and evolutionarily distant species use a similar strategy for thermosensory adaptation. Indeed, we found that zebrafish TRPV1 is activated with a threshold of 32.9 ± 1.2 °C (Supplementary Fig. 14a–d), consistent with physiological adaptation of the animal to its environment of 25–33 °C (ref. 24). When compared to rat TRPV1, the zebrafish channel has a gap of 12 amino acids within the C terminus corresponding precisely to the location of the splice junction in the vampire bat channel (Supplementary Fig. 14e). This gap results from a polymorphism within exon 15 of the zebrafish *trpv1* gene, and thus zebrafish and vampire bats use different mechanisms to generate TRPV1 C-terminal variants.

RNA splicing extends the coding potential of the genome and enhances functionality of the proteome²⁵. The vampire bat uses this strategy to produce physiologically distinct channels, thereby generating

a hypersensitive detector (TRPV1-S) within a specific thermosensory organ, without sacrificing somatic thermo-sensation and/or thermo-nociception. Moreover, our results demonstrate that sequence variation within a specific region of the cytoplasmic C-terminus accounts for differential thermal response profiles of vampire bat TRPV1 isoforms. Indeed, we previously proposed that this region of the channel interacts with membrane phospholipids to modulate sensitivity to thermal and chemical stimuli²⁶.

In addition to illuminating mechanisms of thermosensation and sensory adaptation, the analysis of TRP channel gene structure provides a physiologically relevant marker for assessing phylogenetic relationships. Our findings support recent molecular classification in which bats are grouped together with horses, dogs, cows, moles and dolphins (Laurasiatheria superorder), rather than with humans, monkeys, flying lemur, mouse, rat and rabbits (Euarchontoglires superorder) as originally proposed on the basis of anatomical criteria.

METHODS SUMMARY

Bat tissue was fixed with paraformaldehyde for *in situ* hybridization histochemistry or homogenized in TRIzol for nucleic acid analysis. cDNA libraries were sequenced on Illumina Genome Analyzer II. Cloned channels were transiently expressed in HEK293 cells and subjected to calcium imaging using Fura-2/AM ratiometric dye. *Xenopus* oocytes were cultured, injected with 5 ng of cRNA, and analysed 2–5 d post-injection by two-electrode voltage clamp as described²⁷. Thermal stimulation was applied with a custom-made Peltier device (Reid-Dan Electronics). Temperature thresholds represent the point of intersection between linear fits to baseline and the steepest component of Arrhenius profile, as described²⁸.

Full Methods and any associated references are available in the online version of the paper at www.nature.com/nature.

Received 12 January; accepted 3 June 2011.

- Kurten, L. & Schmidt, U. Thermoperception in the common vampire bat (*Desmodus rotundus*). *J. Comp. Physiol.* **146**, 223–228 (1982).
- Schutt, B. *Dark Banquet: Blood and the Curious Lives of Blood-Feeding Creatures* (Three Rivers Press, 2008).
- Tellgren-Roth, A. *et al.* Keeping the blood flowing — plasminogen activator genes and feeding behavior in vampire bats. *Naturwissenschaften* **96**, 39–47 (2009).
- Campbell, A. L., Naik, R. R., Sowards, L. & Stone, M. O. Biological infrared imaging and sensing. *Micron* **33**, 211–225 (2002).
- Bullock, T. H. & Cowles, R. B. Physiology of an infrared receptor: the facial pit of pit vipers. *Science* **115**, 541–543 (1952).
- Gracheva, E. O. *et al.* Molecular basis of infrared detection by snakes. *Nature* **464**, 1006–1011 (2010).
- Kurten, L., Schmidt, U. & Schafer, K. Warm and cold receptors in the nose of the vampire bat *Desmodus rotundus*. *Naturwissenschaften* **71**, 327–328 (1984).
- Molenaar, G. J. The sensory trigeminal system of a snake in the possession of infrared receptors. II. The central projections of the trigeminal nerve. *J. Comp. Neurol.* **179**, 137–151 (1978).
- Bakken, G. S. & Krochmal, A. R. The imaging properties and sensitivity of the facial pits of pitvipers as determined by optical and heat-transfer analysis. *J. Exp. Biol.* **210**, 2801–2810 (2007).
- Safer, A. B. & Grace, M. S. Infrared imaging in vipers: differential responses of crotaline and viperine snakes to paired thermal targets. *Behav. Brain Res.* **154**, 55–61 (2004).
- Kishida, R., Goris, R. C., Terashima, S. & Dubbeldam, J. L. A suspected infrared-recipient nucleus in the brainstem of the vampire bat, *Desmodus rotundus*. *Brain Res.* **322**, 351–355 (1984).
- Schafer, K., Braun, H. A. & Kurten, L. Analysis of cold and warm receptor activity in vampire bats and mice. *Pflugers Arch.* **412**, 188–194 (1988).
- Caterina, M. J. *et al.* The capsaicin receptor: a heat-activated ion channel in the pain pathway. *Nature* **389**, 816–824 (1997).
- Jordt, S. E., McKemy, D. D. & Julius, D. Lessons from peppers and peppermint: the molecular logic of thermosensation. *Curr. Opin. Neurobiol.* **13**, 487–492 (2003).
- Ramsey, I. S., Delling, M. & Clapham, D. E. An introduction to TRP channels. *Annu. Rev. Physiol.* **68**, 619–647 (2006).
- Black, D. L. Mechanisms of alternative pre-messenger RNA splicing. *Annu. Rev. Biochem.* **72**, 291–336 (2003).
- Will, C. L. & Luhrmann, R. Splicing of a rare class of introns by the U12-dependent spliceosome. *Biol. Chem.* **386**, 713–724 (2005).
- Murphy, W. J. *et al.* Molecular phylogenetics and the origins of placental mammals. *Nature* **409**, 614–618 (2001).
- Murphy, W. J. *et al.* Resolution of the early placental mammal radiation using Bayesian phylogenetics. *Science* **294**, 2348–2351 (2001).
- Nishihara, H., Hasegawa, M. & Okada, N. Pegasoferae, an unexpected mammalian clade revealed by tracking ancient retroposon insertions. *Proc. Natl Acad. Sci. USA* **103**, 9929–9934 (2006).
- Asher, R. J., Bennett, N. & Lehmann, T. The new framework for understanding placental mammal evolution. *Bioessays* **31**, 853–864 (2009).
- Prasad, A. B., Allard, M. W. & Green, E. D. Confirming the phylogeny of mammals by use of large comparative sequence data sets. *Mol. Biol. Evol.* **25**, 1795–1808 (2008).
- Pettigrew, J. D. *et al.* Phylogenetic relations between microbats, megabats and primates (Mammalia: Chiroptera and Primates). *Phil. Trans. R. Soc. Lond. B* **325**, 489–559 (1989).
- Spence, R., Gerlach, G., Lawrence, C. & Smith, C. The behaviour and ecology of the zebrafish, *Danio rerio*. *Biol. Rev. Camb. Phil. Soc.* **83**, 13–34 (2008).
- Grabowski, P. J. & Black, D. L. Alternative RNA splicing in the nervous system. *Prog. Neurobiol.* **65**, 289–308 (2001).
- Prescott, E. D. & Julius, D. A modular PIP2 binding site as a determinant of capsaicin receptor sensitivity. *Science* **300**, 1284–1288 (2003).
- Chuang, H. H., Neuhauser, W. M. & Julius, D. The super-cooling agent icilin reveals a mechanism of coincidence detection by a temperature-sensitive TRP channel. *Neuron* **43**, 859–869 (2004).
- DeCoursey, T. E. & Cherny, V. V. Temperature dependence of voltage-gated H⁺ currents in human neutrophils, rat alveolar epithelial cells, and mammalian phagocytes. *J. Gen. Physiol.* **112**, 503–522 (1998).

Supplementary Information is linked to the online version of the paper at www.nature.com/nature.

Acknowledgements We thank Y. Kelly and J. Poblete for technical assistance, C. Sehnert for help with bovine tissue collection, M. Suzawa and H. Ingraham for providing zebrafish mRNA, A. Walsh for providing megabat blood samples, the Centro Técnico de Producción Socialista Florentino for providing access to Hato Piñero (Cojedes, Venezuela) for animal collection and J. Nassar for providing access to laboratory material required for specimen collection. This work was supported by a Ruth L. Kirschstein National Research Service Award (GM080853; N.T.I.), a Pathway to Independence Fellowship from the UCSF CVRI (E.O.G.), the Howard Hughes Medical Institute (J.S.W.), and grants from NIH, including PO1 AG010770 (J.S.W.) and NS047723 and NS055299 (D.J.).

Author Contributions E.O.G., J.F.C.-M. and N.T.I. designed and performed experiments and analysed data. N.T.I. and J.S.W. developed analytical tools and analysed data. J.A.G.-C., C.I.A. and C.M. collected bat species and obtained tissues for analysis. E.O.G., J.F.C.-M. and D.J. wrote the manuscript with discussion and contributions from all authors. J.S.W. and D.J. provided advice and guidance throughout.

Author Information Deep sequencing data are archived under GEO accession number GSE28243. GenBank accession numbers are JN006855 (*D. rotundus* TRPV1-S), JN006856 (*D. rotundus* TRPV1-L), JN006857 (*D. rotundus* TRPA1), JN006858 (*C. brevicauda* TRPA1), JN006859 (*C. brevicauda* TRPV1-L), JN006860 (*C. brevicauda* TRPV1-S), JN006861 (*Scapanus orarius* TRPV1-L), JN006862 (*S. orarius* TRPV1-S), JN006863 (*Pteropus rodricensis* intron), JN006864 (*D. rotundus* intron), JN006865 (*C. brevicauda* intron), JN006866 (*P. vampyrus* intron), JN006867 (*Rousettus aegyptiacus* intron) and JN006868 (*S. orarius* intron). Reprints and permissions information is available at www.nature.com/reprints. The authors declare no competing financial interests. Readers are welcome to comment on the online version of this article at www.nature.com/nature. Correspondence and requests for materials should be addressed to D.J. (david.julius@ucsf.edu) or to N.T.I. (ingolia@ciwemb.edu) for information concerning bioinformatics.

METHODS

Tissue collection. Vampire bats (*D. rotundus*) and fruit/nectar/insect eating bats (*C. brevicauda*, *A. cultrata*, *U. bilobatum* and *S. lilium*) were collected in pasture forests grazed by cattle at the Hato Piñero ranch, property of the Centro Técnico de Producción Socialista Florentino, located near El Baúl, Cojedes State, Venezuela. Genetic resource and animal sampling permits were obtained from the Ministerio del Ambiente (MINAMB). Global coordinates for animal collection are provided in Supplementary Fig. 15.

Bovine trigeminal ganglia were collected from 12-day old calves for RNA extraction under supervision of C. Sehnert. Blood samples from megabats were generously provided by the Lube Bat Conservatory. A summary of samples from all species examined is provided in Supplementary Fig. 15.

Deep sequencing and analysis. Sequencing libraries were prepared from poly (A)+ RNA using the Illumina mRNA-Seq Sample Prep Kit according to the manufacturer's instructions. Libraries were then sequenced on the Illumina Genome Analyzer II using two 36-cycle sequencing kits to read 80 nucleotides of sequence from a single end of each insert, by standard protocols. Between 7.6 and 26.2 million inserts were sequenced for each sample.

Sequences were aligned to the cow RefSeq protein database (downloaded from NCBI ftp://ftp.ncbi.nih.gov/genomes/Bos_taurus/protein/protein.fa.gz on 25 August 2009) using the blastx tool from NCBI blast (version 2.2.21), which aligns a six-frame translation of each query against a protein database. The alignment was performed with a word size of four amino acids and a window size of five; a maximum *E* value of 1×10^{-5} was required. For each read that aligned to the cow proteome, a set of optimal hits was collected based on alignments whose bit score was within 0.2 of the highest bit score reported for that sequencing read. Each RefSeq alignment for a given sequencing read was converted to an Entrez Gene identifier and redundant alignments for a single read, which correspond to alignments against different isoforms of the same protein, were collapsed to a single count. The number of optimally aligning reads was then counted for each gene; in some cases a single read counted towards several genes.

Splice variants were quantified by aligning sequencing reads to the nucleotide sequence of the alternative TRPV1 isoforms using Bowtie v0.11.3. The alignments were manually inspected to ensure that they supported the splice junction with at least 24 nucleotides aligning on one side of the TRPV1 transcript and at least two nucleotides unambiguously distinguishing the isoform.

The TRPV1 protein sequences were taken from this study, Ensembl (finch, macaque, horse and elephant) and RefSeq (all others), and aligned using t_coffee (ref. 29) in 'accurate' mode with the blosum80mt distance matrix. The protein multiple sequence alignment was used as input to MrBayes³⁰ and the phylogeny was estimated using gamma-distributed substitution rates under the Blosum62 distance matrix combined with a fraction of invariant sites. The phylogeny distribution was estimated across 10 runs, each of 6,000,000 MCMC cycles, with samples every 100,000 cycles following a 1,000,000 cycle burn-in. The chicken and finch sequences were used to root the mammalian tree and are not shown.

Cloning. Functional cDNAs were amplified from first strand cDNA generated by reverse transcription using following primers. Vampire bat *Trpv1* (forward: 5'-GCAAGGATGAAGAAACGGG-3'; reverse: 5'-CCTCACTTTTCCCCTAAA GC-3'). Vampire bat *Trpa1* (forward: 5'-GGCCTGCGTAACATCAGAAGC-3'; reverse: 5'-TACTGCTAAGGTCCTGCATTGTTGG-3'). *C. brevicauda Trpv1* (forward: 5'-CTTGGGCAAAGATGAAGAAACG-3'; reverse: 5'-GTGTGCTAG TCTAAGGCCA-3'). *C. brevicauda Trpa1* (forward: 5'-GCATCCAGGGTAGG ATCCAT-3'; reverse: 5'-CAAGAAACGTGTGTGTGGGA-3'). Zebrafish *trpv1* (forward: 5'-CCTCAAGCCAAGTTACTCAC-3'; reverse: 5'-TCGAAGGACAC CTTGTAGAC-3'). Cow *Trpv1* (forward: 5'-ATGAAGAAATGGGGAGCT CAG-3'; reverse: 5'-TCACTTCTCCCCTAAAGCCAC-3'). Coast mole *Trpv1* (forward: 5'-GGAGCTGGCAAGGATGAAG-3'; reverse: 5'-ATCCTAAGGCC CAACAGAGT-3'). Genomic DNA was extracted from vampire bat (*Desmodus rotundus*) and fruit bat (*C. brevicauda*, *Sturnira bilobatum*) brain, and coast mole

TG, using TRIzol Reagent (Invitrogen); genomic DNA of megabats was extracted from blood using QIAmp DNA Blood mini kit (Qiagen). The genomic region between exon 14 and 15 was amplified using the following primers. Vampire bat, megabats (forward: 5'-CAGGCAATTGTGAAGGCATC-3'; reverse: 5'-CCA GGGCAAAGTCTTCCAG-3'). *C. brevicauda*, *Sturnira bilobatum* (forward: 5'-CGGGCAATTGTGAAGGCAT-3'; reverse: 5'-CCAGGGCAAAGTCTT CCAG-3'). Coast mole (forward: 5'-CTTCTCCCTGCGGTCAAG-3'; reverse: 5'-CTCGAGTGCCTGCATCTCTTAA-3').

Oocyte electrophysiology. Surgically extracted oocytes from *Xenopus laevis* (Nasco) were cultured, injected with 5 ng of RNA, and analysed 4–5 d post-injection by two-electrode voltage-clamp using a Geneclamp 500 amplifier (Axon Instruments, Inc.) as described²⁷. Microelectrodes were pulled from borosilicate glass capillary tubes to obtain resistances of 0.3–0.7 MΩ. Bath solution contained 10 mM HEPES, 120 mM NaCl, 2 mM KCl, 1 mM EGTA and 2 mM MgCl₂ buffered to a final pH of 7.4 with NaOH. Data were analysed using pCLAMP10 software.

Determination of thermal threshold and temperature coefficients (Q₁₀). Temperature thresholds represent the point of intersection between linear fits to baseline and the steepest component of the Arrhenius profile. Values are derived from averages of individual curves; *n* ≥ 8. Arrhenius curve were obtained by plotting the current (+80 mV) on a log scale against the reciprocal of the absolute temperature. Q₁₀ was used to characterize the temperature dependence of the ionic current as calculated using the following equation:

$$Q_{10} = \left[\frac{R_2}{R_1} \right]^{10/(T_2 - T_1)}$$

where *R*₂ is the current at the higher temperature (*T*₂) and *R*₁ is the current at the lower temperature (*T*₁) (ref. 28).

Calcium imaging. All tested channels were transiently expressed in HEK293 cells with the use of Lipofectamin 2000 (Invitrogen). Calcium imaging of HEK293 cells using Fura-2/AM was performed on coverslips coated with Matrigel (BD). Fluorescent images were acquired with Metafluor software (Molecular Devices) and analysed using Graph Pad Prism 4.

In situ hybridization histochemistry. TG and DRG tissue were dissected and fixed in 4% PFA in PBS for 2 d. Cryostat sections (12–15 μm thick) were processed and probed with a digoxigenin-labelled cRNA. Probes were generated by T7/T3 *in vitro* transcription reactions using full length *Trpv1* cDNA and a 3-kb fragment of *Trpa1* cDNA. Signal was developed with alkaline phosphatase-conjugated anti-digoxigenin Fab fragments, according to the manufacturer's instructions (Roche).

In vivo splicing assay. Mini-gene constructs. Genomic region containing vampire bat or *C. brevicauda* splice junction between exon 14–15, exon 14–14a and exon14a–15 was topo-cloned, then subcloned into pcDNA3(+) vector (Invitrogen) using BamHI/XhoI restriction sites. Transfections. HEK293 cells were cultured in DMEM medium supplemented with 10% fetal bovine serum in 6-well plates. At 50% confluence, cells were transiently transfected with 1 μg of mini-gene plasmid or empty pcDNA3 (+) vector using the Lipofectamin method. Cells were harvested 48h after transfection using TRIzol reagent (Invitrogen). cDNA synthesis and RT-PCR. RNA was extracted using TRIzol reagent. RNA (10 μg) was used as template for cDNA synthesis using SuperScriptIII first strand synthesis system (Invitrogen). Synthesis was primed with oligo (dT) or by use of primer annealing to 3'-untranslated sequences in pcDNA3 (CAGTCGAGGCT GATCAGCGAGCT). 5% of cDNA was used in 36-cycle PCR using forward: 5'-TAATACGACTCACTATAGGG-3'; reverse: 5'-CAGTCGAGGCTGATCAG CGAGCT-3' primers. Reaction products were resolved by electrophoresis on 1.5% agarose gel. PCR products were isolated from the gel, cloned into Strataclone vector and sequenced.

29. Notredame, C., Higgins, D. G. & Heringa, J. J., *Mol. Biol.* **302**, 205–217 (2000).

30. Ronquist, F. & Huelsenbeck, J. P. MRBAYES 3: Bayesian phylogenetic inference under mixed models. *Bioinformatics* **19**, 1572–1574 (2003).